Triple-faced polypropylene: Fire retardant, thermally stable, and antioxidative

Henri Vahabi, Seyed Mohammad Reza Paran, Meisam Shabanian, Loïc Dumazert, Rodolphe Sonnier, Elnaz Movahedifar, Payam Zarrintaj, Mohammad Reza Saeb

Triple-Faced Polypropylene: Fire Retardant, Thermally Stable, and Antioxidative

Henri Vahabi [1,2] Seyed Mohammad Reza Paran,[3] Meisam Shabanian,[4] Loïc Dumazert,[5] Rodolphe Sonnier,[5] Elnaz Movahedifar,[6] Payam Zarrintaj,[3,7,8] Mohammad Reza Saeb [1,2,3,9]

[1]*Université de Lorraine, CentraleSupélec, LMOPS, F-57000 Metz, France*

[2]*Laboratoire Matériaux Optiques, Photoniques et Systèmes, CentraleSupélec, Université Paris-Saclay, 57070 Metz, France*

[3]*Advanced Materials Group, Iranian Color Society, Tehran, Iran*

[4]*Faculty of Chemistry and Petrochemical Engineering, Standard Research Institute, Karaj, Iran*

[5]*Ecole des Mines d'Alès, Centre des Matériaux des Mines d'Alès—Pôle Matériaux Polymères Avancés, 6 Avenue de Clavières, 30319 Alès CEDEX, France*

[6]*Department of Polymer Engineering, Amirkabir University of Technology–Mahshahr Campus, Mahshahr, Iran*

[7]*Polymer Engineering Department, Faculty of Engineering, Urmia University, Urmia, Iran*

[8]*Department of Polymer Engineering and Color Technology, Amirkabir University of Technology, Tehran, Iran*

[9]*Department of Resin and Additives, Institute for Color Science and Technology, Tehran, Iran*

A halogen-free nitrogen-rich additive was used to make polypropylene (PP) prepared for three different missions: fire retardancy, thermal stability, and antioxidative properties. The prepared additive was composed of a cyclodextrin, a nanohydroxyapatite, and a poly[[6-[(1,1,3,3,-tetramethylbutyl)amino]-1,3,5-triazine-2,4-diyl][(2,2,6,6-tetramethyl-4-piperidinyl)imino]-1,6-hexanediyl[2,2,6,6-tetramethyl-4-piperidinyl)imino] (SABO®STAB) integrated into a unique molecule, namely, BSDH. Fire retardancy performance of BSDH in PP was compared with that of 9,10-dihydro-9-oxa-10-phosphaphenanthrene-10-oxide (DOPO) commercially available additive in terms of cone calorimeter results. Thermal stabilities of PP/BSDH and PP/DOPO composites were compared by changes observed in pyrolysis activation energy values measured in thermogravimetric analysis under nitrogen atmosphere at various heating rates. Flame retardancy of PP/BSDH composite was reflected in a drop in the peak of Heat Release Rate by *ca.* 31% with respect to neat PP. Very interestingly, the results show that BSDH additive retarded thermal oxidation of PP macromolecular chains when compared with DOPO commercially available flame retardant, as signaled by a rise in oxidation induction time value as well as an increased early-stage activation energy needed for thermal decom-position of PP in the presence of BSDH.

Correspondence to: H. Vahabi; e-mail: henri.vahabi@univ-lorraine.fr or M. R. Saeb; e-mail: saeb-mr@icrc.ac.ir

INTRODUCTION

Development and commercialization of new grades of polymers is economically challenging. There are serious challenges with sustainability considerations as well, which highlight the importance of green techniques for blending of polymers with additives while keeping the process profitable and the performance of the resulting composites polymer sufficiently high for engineering applications. In this sense, researchers are attempting to bridge the gap between needs for high-performance plastics and their materialization by giving value to the addition of additives to general-purpose plastics. Ever-increasing demand for high-performance plastics has opened new windows to achieve new classes of reinforced plastics by the addition of multifunctional additives to commodity plastics [1–3]. Fire retardancy of different thermoplastic [4–6] and thermosetting [7,8] systems containing various additives was the focus of recent studies.

Polypropylene (PP)-based commodity plastics are known for their excellent mechanical properties, antibacterial nature, biocompatibility, lightweight, and more promisingly their low cost [9,10]. The demand for PP is estimated to reach *ca.*

62 million tons by 2020 [11]. Despite above-mentioned advantages and market necessities, PP suffers from a high fire risk because of its inherent flammable character. The flammability is a constraint that limits the usage of PP in construction and electric and electronic applications [12]. Therefore, the development of effective and environmentally friendly flame retardants for PP has received a great deal of attention [13,14]. It is also worth mentioning that development of flame-retardant PP is of interest bearing in mind new regulations and legislations from safety, environmental, and toxicological perspectives [15].

A number of solutions have been already examined to improve the fire retardancy of PP, which can be treated in physical (using additives) and chemical (using reactive precursors) routes [16,17]. From degradation point of view, PP is sensitive to oxidation; therefore, it is essential to use suitable antioxidants in PP formulations [18]. Oxidation unavoidably takes place during PP melt processing as well as over its life cycle. From an industrial standpoint, however, one may need to combine properties of different additives to gain a "multifunctional" additive that may bring about several benefits to PP polymer. The use of a multifunctional additive rather than mixture of additives with different functionalities leads to facilitation of processing and facile dispersion of additives into the molten polymer [19]. Therefore, there has been a great deal of research to find appropriate ways for tailoring properties of different additives into a unique versatile additive as the next generation of high-performance multifunctional derivatives—what brings about new challenges in spite of being interesting [20].

In a recent work, a flame retardant was developed and applied in poly(lactic acid) (PLA) showing an acceptable efficiency [21]. This flame retardant was the hybrid product of the reaction between three different molecules: β-cyclodextrin, nanohydroxyapatite, and an antioxidant (commercially available SABO®), and named BSDH in brief [20]. In view of successfulness of the BSDH as a flame retardant for PLA, we were anxious to uncover its potential toward PP as a flame retardant and at the same time as an antioxidation agent. Such a dual functionality would be expected in view of a report suggesting that N-alkoxy-hindered amines can play the role of flame retardant and has synergistic effect between the developed precursor and conventional flame retardants due to free-radical quenchability and high flame-retardant efficiency of the developed precursor [22–25]. Besides, recently, 9,10-dihydro-9-oxa-10-phosphaphenanthrene-10-oxide (DOPO) is presented as a new and effective flame retardant, and several papers reported the use of DOPO in PP [26–29]. Overall, there is evidence that the presence of 1.5–2 wt% phosphorus element in the system is adequate to reach an acceptable level of flame retardancy. Considering the fact that the percent-age of phosphorus in commercial DOPO was around 14%, incorporation of 10 wt% of DOPO into polymer could be justified, giving *ca.* 1.5 wt% phosphorous as a whole. In addition, a glimpse at the literature shows that in majority of works, DOPO incorporation has been fixed at around 10 wt% [30–32]. In the light of above discussions and evidences, this work seeks to uncover the performance of BSDH as a trifunctional flame retardant with antioxidant action in PP matrix by comparing its performance with DOPO. First, a code was developed in MATLAB media to calculate kinetic activation energy of the system as a function of mass loss during thermogravimetric analysis (TGA) under different heating rates to recognize the mechanism behind which BSDH precursor might stabilize PP against thermal degradation. Then, samples contain 10 wt% of BSDH or DOPO melt-blended and characterized by TGA, differential scanning calorimetry (DSC), and cone calorimetry. A mechanistic description of thermal degradation was proposed based on activation energy calculation and speculations behind fire scenario used.

THEORETICAL AND EXPERIMENTAL ANALYSES

Theory on Thermal Decomposition Analysis

Network formation and network degradation are two possible cases, respectively, taking place by the release and receive of thermal energy. Designing advanced materials/systems with specific functions requires application of well-documented criteria for optimization [33–36]. Addition of additives changes thermal characteristic of polymer systems, where mathematical modeling can bring about useful insights about events taking place in molecular level [37–40]. Introduction of flame-retardant additives changes thermal stability and thermal decomposition behavior of polymers. TGA has been widely used for obtaining the kinetic parameters such as reaction model, $f(\alpha)$ preexponential factor, and activation energy, and E_α to deepen understanding of thermal decomposition mechanism of polymers [41,42]. In a recent work, we comprehensively explained the methodology and applied it for a very complex case containing a thermoplastic, a rubber, and a nanoparticle [43]. Two mathematical approaches are generally applied in finding kinetic parameters from thermogravimetric [44] or differential calorimetric data, [45–47] and the model-fitting and model-free (isoconversional) approaches. TGA measurements can be performed under isothermal or nonisothermal conditions. However, in "model-free" isoconversional methods, which are more reliable for assessing complex mechanisms such as thermal decomposition of polymers, nonisothermal routes can be satisfactorily used to obtain the E_α as a function of the mass loss, α and bring more useful insights into the kinetics of thermal decomposition [48].

Kinetics of thermal decomposition of polymers can be expressed by the general form defined as *Eq. 1*:

$$\frac{d\alpha}{dt} = k(T)f(\alpha) \tag{1}$$

so that α takes values in the interval [0, 1], t is the time, $k(T)$ is the rate constant of decomposition reaction, and $f(\alpha)$ is representative of the mass loss. The temperature dependence $k(T)$ is described as follows on the basis of Arrhenius equation[49]:

$$k(T) = Aexp\left(-\frac{E_a}{RT}\right) \tag{2}$$

where A is the preexponential factor, R is the universal gas constant, and E_α is the activation energy of thermal

decomposition. The partial mass loss α in a thermal decomposition is defined as:

$$\alpha = \frac{(W_0 - W_t)}{(W_0 - W_f)} \quad (3)$$

where W_0 is the initial weight of the sample, W_t is the weight of the sample at time t, and W_f is the final weight remained after degradation. By the substitution of *Eq. 2* into *Eq. 1*, the rate of thermal decomposition can be described as:

$$\frac{d\alpha}{dt} = A exp\left(-\frac{E_a}{RT}\right) f(\alpha) \quad (4)$$

For an *n*th-order decomposition reaction, the above equation can be represented as [50]:

$$\frac{d\alpha}{dt} = A exp\left(-\frac{E_a}{RT}\right) (1-\alpha)^n \quad (5)$$

For nonisothermal TGA data, introducing the heating rate $\beta = dT/dt$ in *Eq. 4* leads to the following equation, which is the fundamental expression for the calculation of the kinetic parameters of thermal decomposition:

$$\frac{d\alpha}{dT} = \left(\frac{A}{\beta}\right) exp\left(-\frac{E_a}{RT}\right) f(\alpha) \quad (6)$$

Since decomposition of polymers has a complex kinetics that cannot be demonstrated with a single equation at the whole temperature rage, it is recommended to use a model-free isoconversional method, which assumes that at a constant mass loss, the rate of thermal decomposition is solely a function of the temperature [50–52].

Kissinger–Akahira–Sunose kinetics model is an integral form of the isoconversional methods, which can make possible the prediction of the activation energy of the reaction by using the following relation [53–55]:

$$\ln\left(\frac{\beta_i}{T_{\alpha,i}^{1.92}}\right) = Const. - 1.0008\left(\frac{E_\alpha}{RT_\alpha}\right) \quad (7)$$

The relation between $\ln\left(\frac{\beta_i}{T_{\alpha,i}^{1.92}}\right)$ and $1/T$ is a straight line that gives the E_α from the slope of the plot.

The isoconversional Ozawa–Flynn–Wall method is another integral method for the calculation of E_α from the slope of $ln(\beta_i)$ with respect to $1/T_\alpha$ at any certain partial mass loss [46,56]. This method is defined as the following equation:

$$\ln(\beta_i) = Const - 1.052\left(\frac{E_\alpha}{RT_\alpha}\right) \quad (8)$$

The modified Coats–Redfern has a nonisothermal basis and has been used for the determination of thermoanalytical rate, which is defined as [57–59]:

$$\ln\left[\frac{\beta}{T^2(1-2RT/E_\alpha)}\right] = \ln\left[\frac{-AR}{E_\alpha \ln(1-\alpha)}\right] - \frac{E_\alpha}{RT} \quad (9)$$

The activation energy can be calculated from the slope of straight lines resulted from plotting the left-hand side of *Eq. 9* for each heating rate against *1/T*. It should be noted the full solution of the above equation needs an iterative method with the first assuming value of E_α. [60] Nevertheless, when using this equation, some precautions should be taken into account [61].

A schematic flowchart on the steps taken in thermal degradation analysis applied on nonisothermal TGA data based on the code written in MATLAB media is demonstrated in Fig. 1. Accordingly, the first step to be taken is to sort the TGA experimental data in the matrix form in the MATLAB software. Then, the matrix will be accepted by the MATLAB code as input data. After that, data processing is done to estimate thermal degradation kinetic parameters such as activation energy, decomposition reaction order, and preexponential factor. The ability of each theoretical model to predict the derivative curves of TGA, that is, named DTG curve of each sample, is represented in terms of kinetic parameters.

Experimental

Materials. PP, SABIC® PP 505P, was provided by Sabic Co. A flame-retardant additive, DOPO was purchased from Tokyo Chemical Industry Co. Details on the synthesis and characterization of trifunctional flame-retardant additive, named BSDH, can be found in a previous paper of this group [21]. Briefly, BSDH was synthesized by integrating a nitrogen-rich polymer (poly[[6-[(1,1,3,3,-tetramethylbutyl) amino]-1,3,5-triazine-2,4-diyl][(2,2,6,6-tetramethyl-4-piperidinyl)imino]-1,6-hexanediyl[2,2,6,6-tetramethyl-4-piperidinyl) imino] SABO®STAB), a cyclodextrin, and a nanohydroxyapatite into a unique molecule.

Preparation of Composites. PP composites were prepared *via* melting processing. The PP pellets were melt-blended for 6 min with BSDH or DOPO in an internal mixer apparatus (HAAKE) at 170°C and a rotor speed of 60 rpm. The names and formulations of samples are given in Table 1. All blends were ground after mixing and then hot-pressed and molded by Agila machine under 60 bars at 180°C for 6 min into specimens in the form of square sheets (100×100×4 mm^3) for cone calorimeter and thermal analyses.

Characterization. TGA was performed on a Setaram Labsys Evo thermogravimetric analyzer at a heating rate of 10°C min^{-1}. The weight of samples in this test was approximately 20 mg. Analyses were carried out in a temperature range of 25–800°C, under a nitrogen flow rate of 50 mL min^{-1}. Flame retardancy parameters including peak of Heat Release Rate (pHRR), time to ignition (TTI), and total heat release (THR) were obtained by doing cone calorimeter

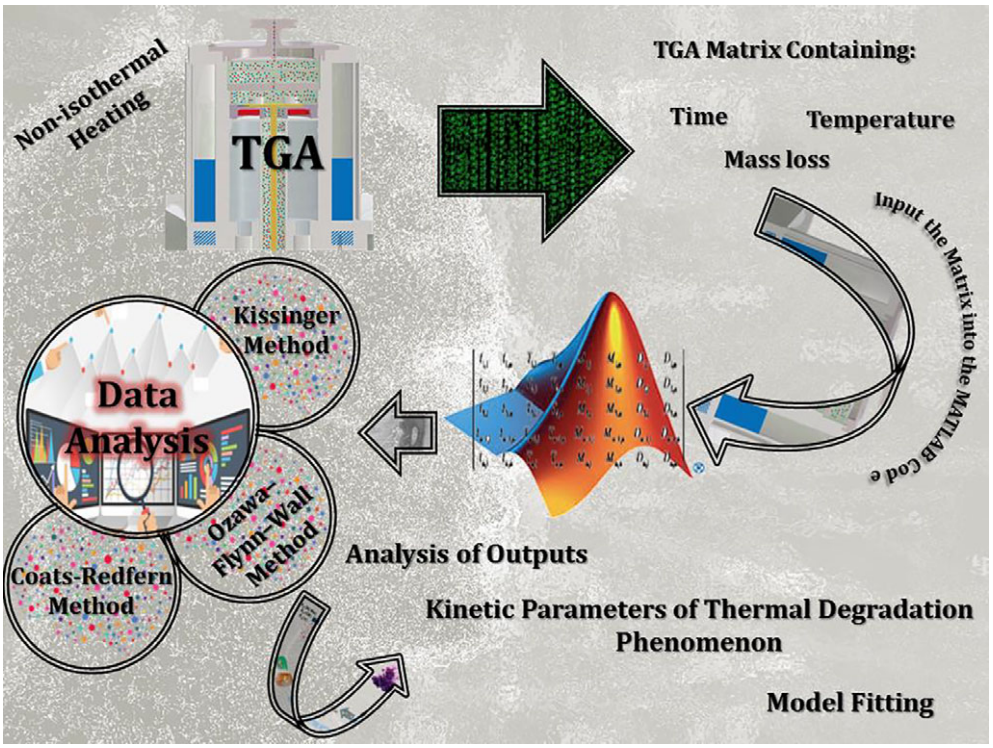

FIG. 1. Procedure used to treat TGA data in order to calculate thermal degradation kinetic parameters. [Color figure can be viewed at wileyonlinelibrary.com]

measurement on an FTT-EU-ISO5660 apparatus. The heat flux was fixed at 35 kW m^{-2}.

Oxidation induction time (OIT) measurements were performed on a DSC 92 from Setaram according to the ISO 11357-6:2013. To do so, samples of about 10 mg (± 1 mg) were placed into a 120-µL aluminum crucible without cover and were heated from 30 to 190°C at 20°C min^{-1} and kept at that temperature for 3 min under nitrogen (30 mL/min). After that, the nitrogen atmosphere was replaced by air (30 mL/min) and the oven was maintained at this temperature for a maximum duration of 2 h. The OIT corresponds to the time between the passage under oxidizing atmosphere and the onset of the exothermic peak. Each sample was analyzed at least three times and the average is reported.

RESULTS AND DISCUSSION

Thermogravimetric Analysis

The TGA and DTG curves of PP, PP/DOPO, and PP/BSDH samples under nitrogen are presented in Fig. 2 and the corresponding data are listed in Table 2. It is apparent that all samples exhibited single-stage decomposition around 460°C under nitrogen demonstrating unimodal decomposition mechanism. The onset temperature ($T_{5wt\%}$) of PP was decreased from 421 to 303°C in the presence of DOPO, while the one for PP/BSDH sample was similar to that of neat PP. Moreover, data in Table 2 suggest that there is no char residue for PP and PP/DOPO samples remained at the end of the test under nitrogen atmosphere, against 6 wt% detected for PP/BSDH sample.

TABLE 1. Name and composition of PP-based composites containing DOPO and BSDH

Sample code	PP (wt%)	DOPO (wt%)	BSDH (wt%)
PP	100	0	0
PP/DOPO	90	10	0
PP/BSDH	90	0	10

Cone Calorimeter Tests

The cone calorimeter is a well-known bench-scale apparatus for assessing fire resistance of materials. It provides several key parameters related to fire scenario and then enables one to track and visualize the combustion behavior of a material. Figure 3 shows the heat release rate (HRR) curves for all samples and the related data are summarized in Table 3. After ignition at 68 s, neat PP quickly burned so that its pHRR reached 1,026 kW m^{-2}, and at the end of test, there was no char residue remained (Fig. 4). For PP/DOPO sample, however, the pHRR decreased to 648 kW m^{-2}, while its TTI was similar to that of pure PP. Incorporation of BSDH led to a fall in TTI down to 32 s. The pHRR of PP/BSDH was relatively similar to that of PP/DOPO sample, 708 kW m^{-2}. However, a meaningful difference was observed between THR values of PP/DOPO (141 MJ m^{-2}) and PP/BSDH (156 MJ m^{-2}) samples. The origin of this difference may be taken in higher contribution of BSDH to heat release because of its structure that contains more chemical groups than DOPO. In contrast to the PP/DOPO sample, a char residue was remained for the PP/BSDH

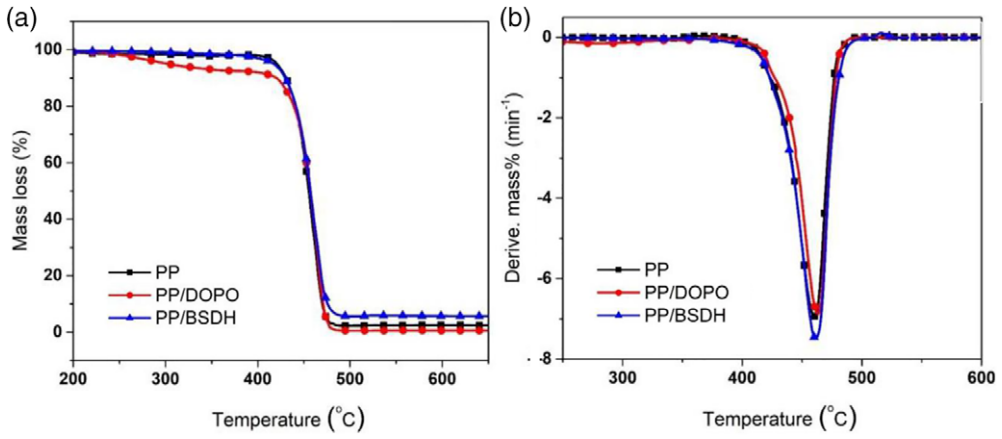

FIG. 2. (a) TGA and (b) DTG curves of PP and its composites collected under nitrogen atmosphere. [Color figure can be viewed at wileyonlinelibrary.com]

sample (Fig. 4). According to these results, it can be concluded that BSDH can appropriately compete at fire prevention with commercially available DOPO additive. Additionally, however, the difference between remaining char observed at the end of cone calorimetry test is a positive point for BSDH as flame retardant, which is explored in this work. Even if a remaining char residue was obtained in the case of PP/BSDH sample, its quality and thickness was not sufficient to prevent the release of gases during combustion. Therefore, the release of gases was led to the formation of cracks, as can be observed in Fig. 4.

TABLE 2. Thermal decomposition data for PP and its composites collected under nitrogen atmosphere

Sample	$T_{5wt\%}$ (°C)	T_{max} (°C)	Residue yield (wt%)
PP	421	460	0
PP/DOPO	303	463	0
PP/BSDH	417	461	6

T_{max}: peak temperature at maximum decomposition rate obtained from DTG curves.

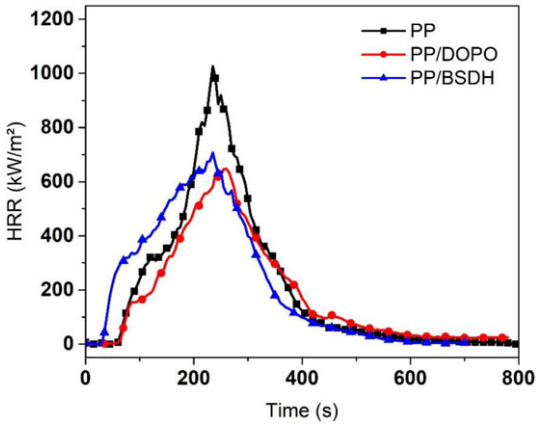

FIG. 3. HRR curves of PP, PP/DOPO, and PP/BSDH samples (irradiance flux: 35 kW m^{-2}). [Color figure can be viewed at wileyonlinelibrary.com]

Oxidation Induction Time Measurement

The lifetime of a polymer is often related to its resistance against oxidative decomposition [62]. The oxidation can take place during melt processing of polymer or even by aging, leading to the deterioration of properties of polymers. It is well known that PP is highly sensitive to oxidation and suffers from chain scission [63,64]. Therefore, it is important to estimate the oxidative decomposition resistance of PP in the presence of additives. The OIT measurement by DSC is a well-known method and gives an index to estimate the oxidative stability of material [65,66]. The procedure used for OIT measurements is schematically sketched in Fig. 5.

As the OIT value increases, the oxidative stability of material mildly increases. Figure 6 shows the curves obtained from OIT test. PP/BSDH sample resisted against oxidation for a longer time up to *ca.* 60 min, while the OIT values of PP and PP/DOPO samples were almost the same at *ca.* 10 min. Therefore, it is apparent that the presence of BSDH significantly increases the oxidative stability of PP compared with commercially available DOPO.

Kinetics of Thermal Decomposition

Figures 7–9 display isoconversional plots obtained for PP, PP/DOPO, and PP/BSDH samples, using Kissinger–Akahira–Sunose, Ozawa–Flynn–Wall, and modified Coats–Redfern methods, respectively. The results are indicative of appropriate curve fitting irrespective of the method, particularly for mass loss values among $\alpha = 0.4$ and $\alpha = 0.9$. As a whole, the outcomes of models are very similar to each other,

TABLE 3. Data extracted from Fig. 4 on cone calorimeter results of the studied samples

Sample code	TTI (s)	pHRR (kW m^{-2})	THR (MJ/m^2)
PP	61	1,026	166
PP-DOPO	60	648	141
PP-BSDH	32	708	156

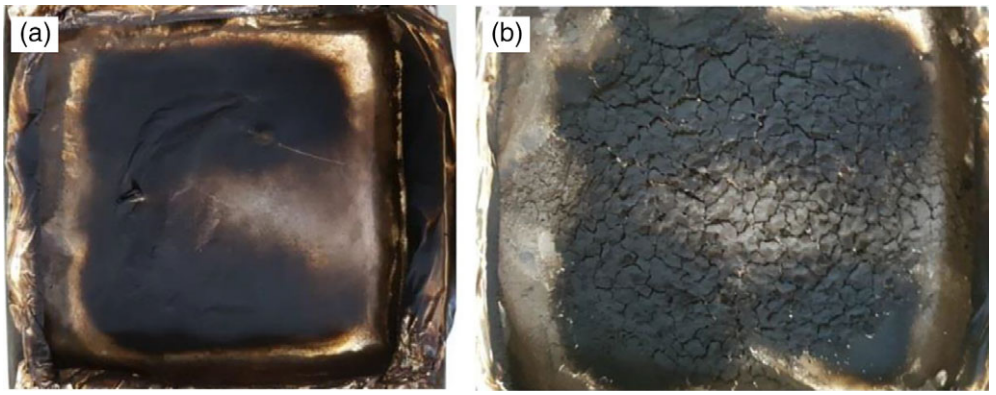

FIG. 4. Digital photographs of the residues remained after cone calorimeter test taken from (a) PP/DOPO and (b) PP/BSDH composites. [Color figure can be viewed at wileyonlinelibrary.com]

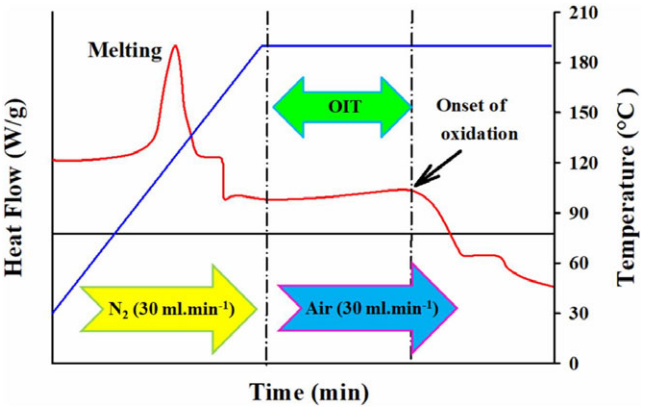

FIG. 5. Principle sequence of OIT measurements. [Color figure can be viewed at wileyonlinelibrary.com]

demonstrating a simple degradation mechanism taking place in the system. Occurrence of this phenomenon was signaled by one-stage decomposition in TGA curves (Fig. 2). It is also interesting to note that plots obtained for PP/BSDH system follow a straight line even for $\alpha < 0.4$ in parallel suggesting the independence of activation energy on mass loss [56,67].

The values of E_α corresponding to thermal decomposition of the studied samples obtained by TGA measurement at different heating rates under nitrogen atmosphere in terms of partial mass loss calculated from the slopes of lines in Figs. 7–9 for three isoconversional models are plotted in Fig. 10. The averages of values of E_α, the preexponential factors, and order of decomposition reaction corresponding to the three methods used in this study are also presented in Table 4.

The trends in E_α variations are nearly close to each other irrespective of the used method. At early stages of thermal decomposition, that is, for partial mass loss values below 0.4, the E_α of PP is obviously less than those of PP/DOPO and PP/BSDH, Interestingly the E_α values in such mass loss zone for PP/BSDH sample take the maximum values compared with the other two samples. By continuation of TGA test, the E_α of PP and PP/BSDH reached more or less a constant value up to the end of test, while that of PP/DOPO experienced a sharp decline at $\alpha = 0.2$–0.6. Further evidence would be provided by comparing the values of the order of decomposition reactions, n given in Table 4, which is indicative of acceleration of thermal decomposition of PP in the presence of DOPO. For instance, the modified Coats–Redfern suggests that n increased from 1.25 for the neat PP to 1.50 for the PP/DOPO sample, demonstrating accelerated decomposition of PP/DOPO compared with PP due to excessive degradation. On the other hand, the value of n for

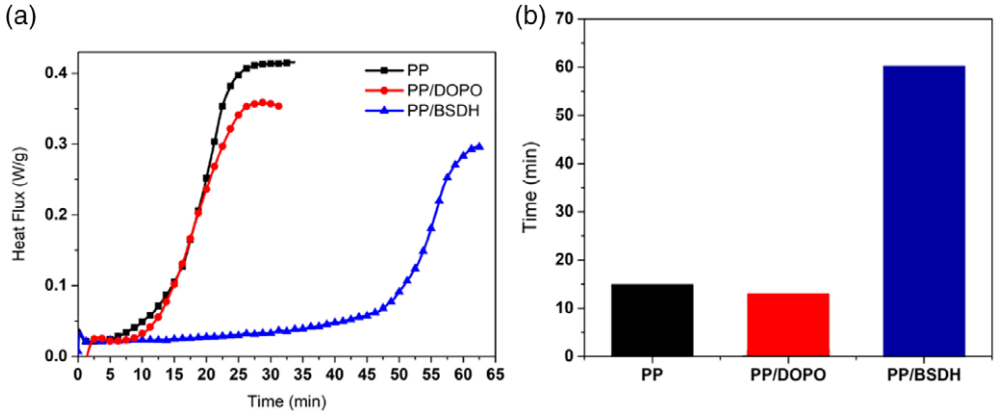

FIG. 6. (a) Time-dependent heat flux and (b) time to oxidation startup obtained from OIT tests performed at 190°C for PP and composite samples. [Color figure can be viewed at wileyonlinelibrary.com]

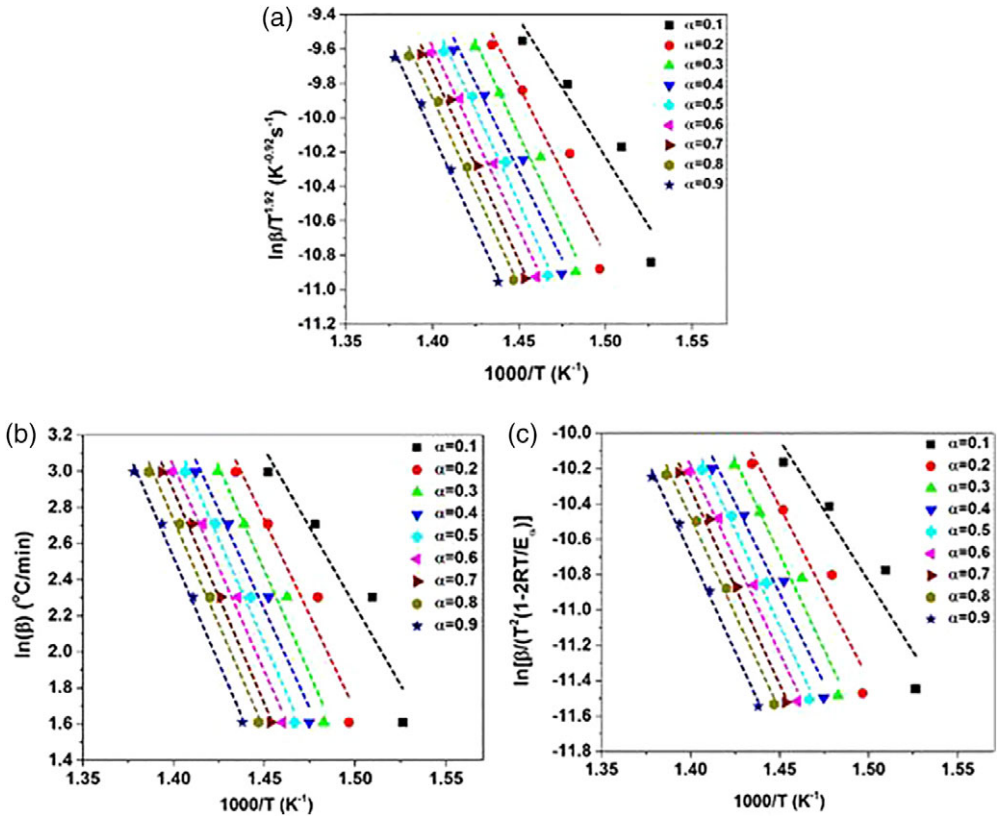

FIG. 7. Typical isoconversional plots for PP obtained using (a) Kissinger–Akahira–Sunose, (b) Ozawa–Flynn–Wall, and (c) modified Coats–Redfern methods applying TGA data obtained at different heating rates under nitrogen atmosphere. [Color figure can be viewed at wileyonlinelibrary.com]

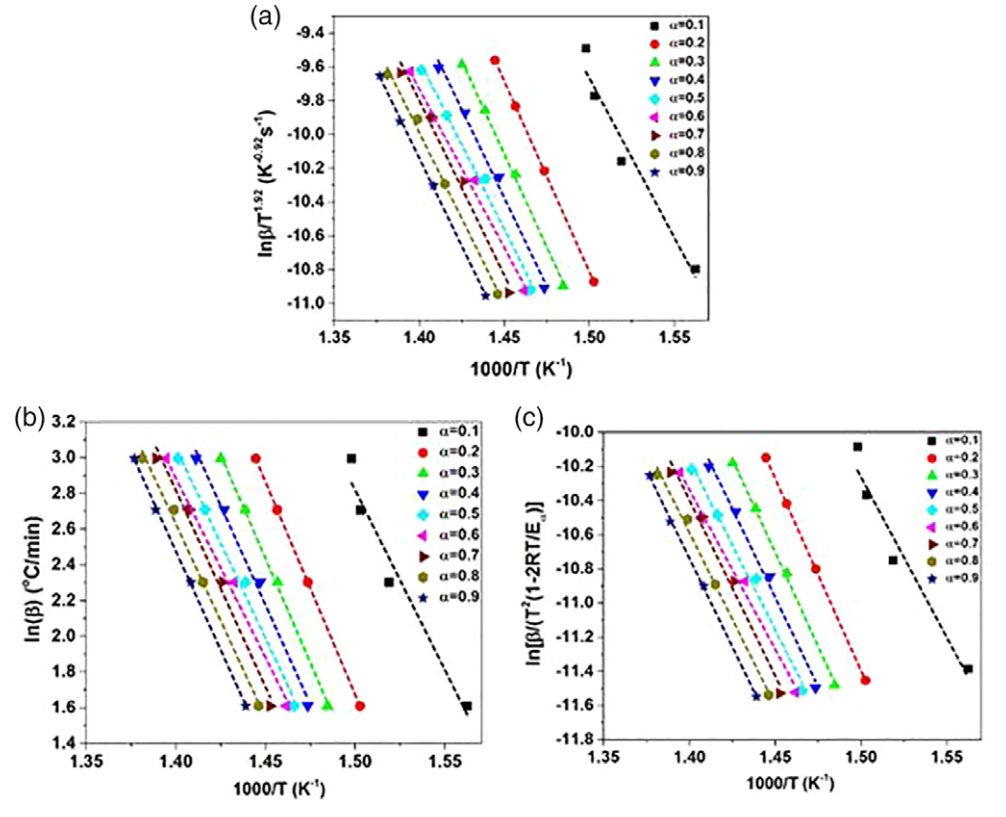

FIG. 8. Typical isoconversional plots for PP/DOPO obtained using (a) Kissinger–Akahira–Sunose, (b) Ozawa–Flynn–Wall, and (c) modified Coats–Redfern methods applying TGA data obtained at different heating rates under nitrogen atmosphere. [Color figure can be viewed at wileyonlinelibrary.com]

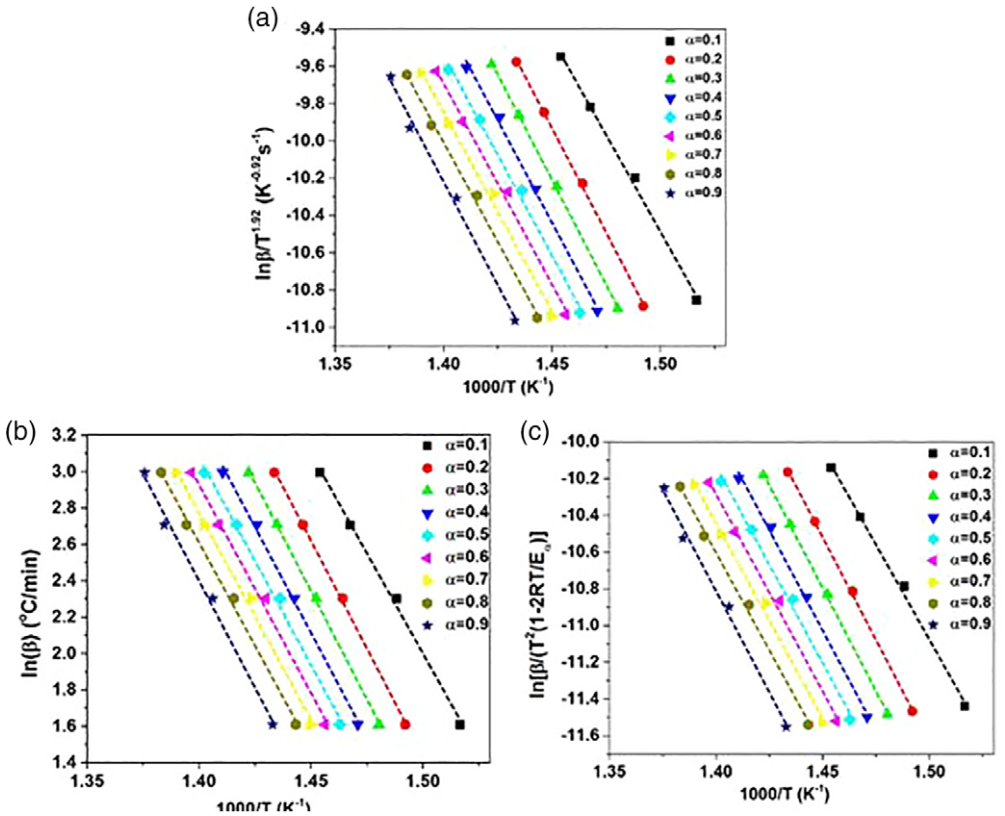

FIG. 9. Typical isoconversional plots for PP/BSDH obtained using (a) Kissinger–Akahira–Sunose, (b) Ozawa–Flynn–Wall, and (c) modified Coats–Redfern methods applying TGA data obtained at different heating rates under nitrogen atmosphere. [Color figure can be viewed at wileyonlinelibrary.com]

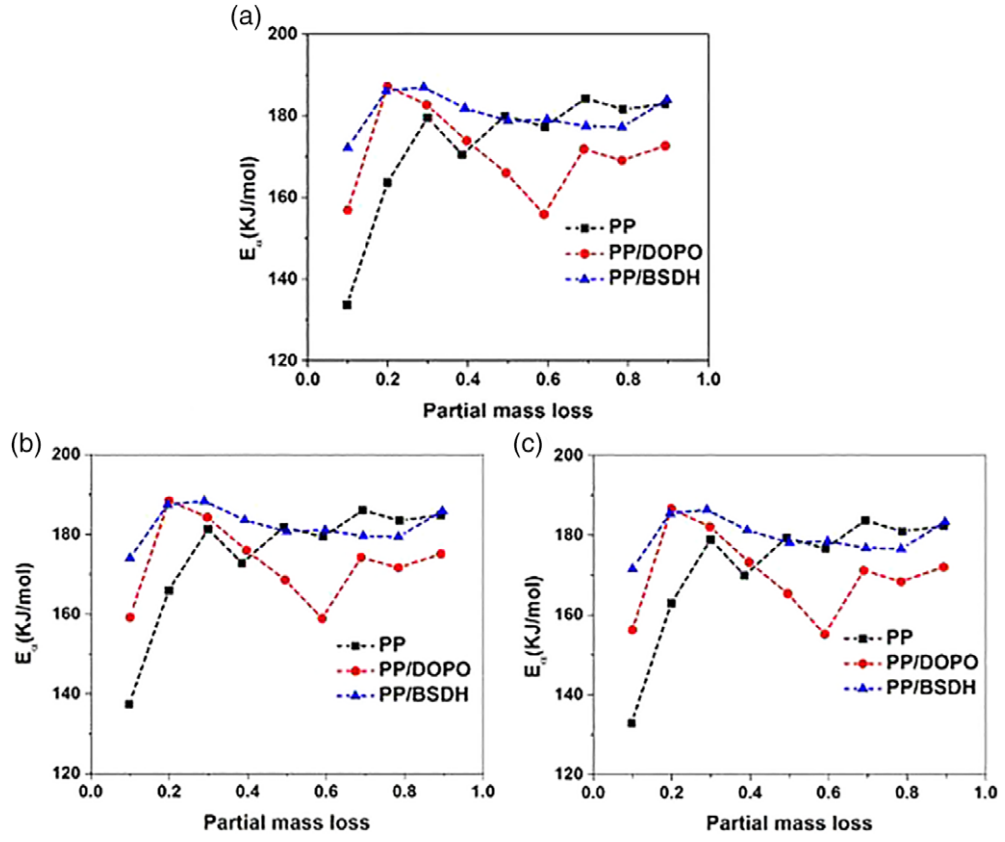

FIG. 10. Activation energy of thermal decomposition for the studied samples as a function of partial mass loss calculated by using (a) Kissinger–Akahira–Sunose, (b) Ozawa–Flynn–Wall, and (c) modified Coats–Redfern methods. [Color figure can be viewed at wileyonlinelibrary.com]

TABLE 4. Average values of E_α in kJ/mol, preexponential factors, and order of decomposition reactions calculated using isoconversional kinetic models over the interval α = 0.1–0.9

Designation	Kissinger–Akahira–Sunose			Ozawa–Flynn–Wall			Modified Coats-Redfern		
	E_α (kJ/mol)	Ln (A) (min^{-1})	N	E_α (kJ/mol)	Ln (A) (min^{-1})	n	E_α (kJ/mol)	Ln (A) (min^{-1})	n
PP	172.67	25.14	1.25	174.80	25.51	1.24	171.93	25.01	1.25
PP/DOPO	170.76	24.91	1.49	172.95	25.28	1.47	170.02	24.78	1.50
PP/BSDH	180.46	26.41	1.21	182.23	26.72	1.21	179.74	26.28	1.22

PP/BSDH was 1.22 implying antithermal decomposition action of BSDH additive developed in this work. A similar trend can be seen among the studied samples irrespective of isoconversional method used. Correspondingly, the average value of frequency factor, *lnA* for PP/BSDH sample is higher than those of PP and PP/DOPO, a criterion that suggests resistance of PP/BSDH sample against thermal degradation.

Random chain scission and intermolecular radical transfer are two main possible events taking place in thermal degradation of PP [68,69] (Fig. 11). The presence of weak bonds in the main chain of PP due to the presence of tertiary carbon atoms is responsible for degradation of PP at early stages of thermal treatment [70]. In agreement with this speculation, the E_α value of PP at the beginning of degradation takes a very low value (Fig. 10). Such a low activation energy at the beginning of degradation can be explained by the initiation of degradation of the inherent weak links such as head-to-head links, [71,72] which is mechanistically explained in Fig. 11. Afterward, higher activation energy is needed to break C—C bonds, as can be obviously observed in Fig. 10 by a sudden rise in the value of E_α up to $\alpha = 0.3$ in PP plot.

Figure 12 displays a mechanism to demonstrate the action of the BSDH bifunctional additive in the PP matrix featured by a rise in the value of E_α. At the beginning of thermal decomposition, free radicals are formed through β-scission of PP chains by the combined actions of heat [73], so as to accelerate the degradation of PP matrix. Simultaneously, the nitroxyl radicals generated upon thermal decomposition of BSDH may quench PP macroradicals as well as other free radicals created through the decomposition of PP that might suppress the degradation of PP [74]. This mechanism is illustrated in Fig. 12.

In the light of above discussions, it can be concluded that such a difference between actions of DOPO and BSDH can be explained by the well-known activity of the hindered amine present in the SABO structure used in preparation of BSDH [21]. Such an action could be pronounced at the early stages of thermal decomposition, where the activity of SABO toward prevention of PP chain scission was featured by capturing free radicals formed in the initiation state. Thus, it can be corroborated that BSDH acts better than the DOPO; therefore, the activation energy of PP/BSDH took higher values than that of PP/DOPO at a full range of mass loss.

CONCLUSIONS

In the present study, a novel flame-retardant system made of β-cyclodextrin, triazine ring, and nanohydroxyapatite (BSDH) was developed and applied in order to improve both flame retardancy and thermal stability characters of PP. The obtained results were compared with those of a commercially available flame retardant (DOPO). First, TGA results showed that thermal stability of PP/BSDH is similar to that of neat PP, but better than that of PP/DOPO sample. Moreover, BSDH (6.0 wt%) yielded char residue in opposition to neat PP (0.0%) and DOPO (0.0%). Second, the performance of BSDH in terms of peak of HRR in cone calorimeter test was similar to that of DOPO in PP. The OIT

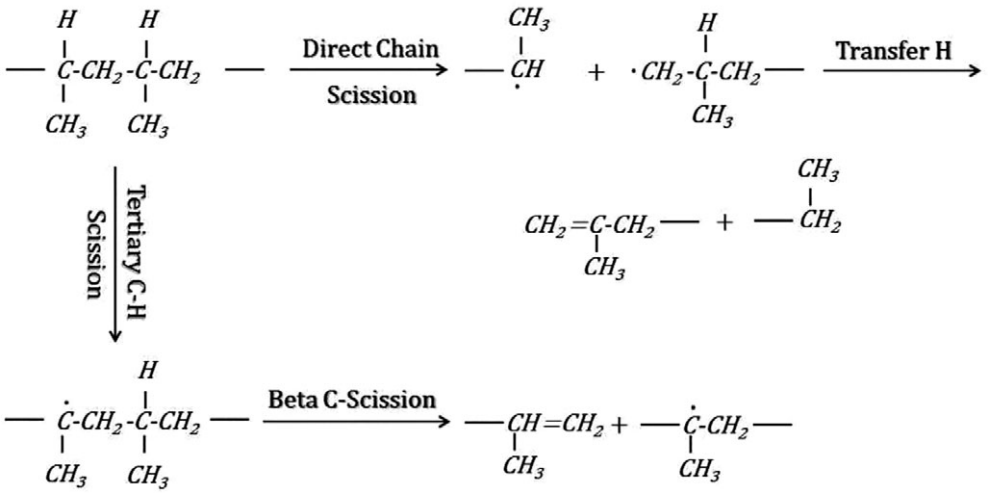

FIG. 11. Mechanism proposed for thermal degradation of PP chain during TGA test.

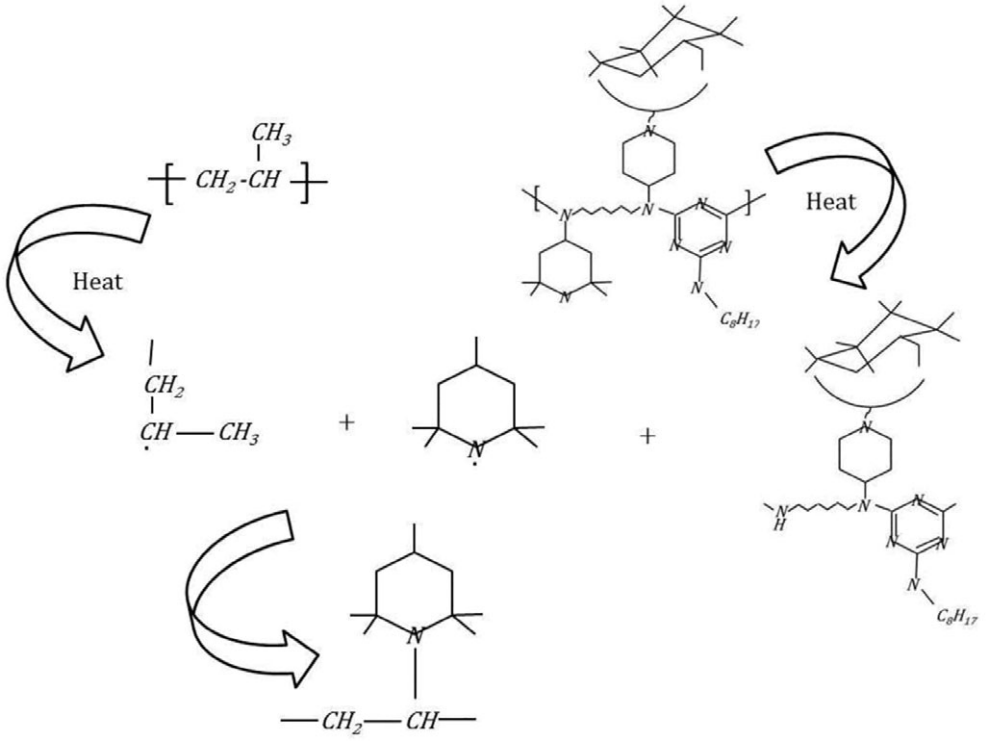

FIG. 12. Possible mechanism of action of BSDH as a thermal stability modifier in PP matrix.

measurement showed the efficiency of BSDH against oxidative decomposition of PP, as the OIT value increased from 15 to 60 min in the presence of BSDH. The activation energy value of thermal decomposition under nitrogen was calculated using a house-written code by Kissinger–Akahira–Sunose, Ozawa–Flynn–Wall, and the modified Coats–Redfern methods. The results demonstrated higher activation energy at the beginning of thermal degradation in the presence of BSDH than DOPO. A possible mechanism was suggested in order to illustrate the action of BSDH in quenching the PP macroradicals, and consequently increase the activation energy value.

DATA AVAILABILITY

The raw/processed data required to reproduce these findings cannot be shared at this time as the data also form part of an ongoing study.

REFERENCES

1. J.-F. Lutz, J.-M. Lehn, E. Meijer, and K. Matyjaszewski, *Nat. Rev. Mater.*, **1**, 16024 (2016).
2. N. Zafeiropoulos, D. Williams, C. Baillie, and F. Matthews, *Compos. Part A Appl. Sci. Manuf.*, **33**, 1083 (2002).
3. S. Mohebbi, M.N. Nezhad, P. Zarrintaj, S.H. Jafari, S. S. Gholizadeh, M.R. Saeb, and M. Mozafari, *Curr. Stem Cell Res. Ther.*, **13**, 93 (2019).
4. F. Laoutid, H. Vahabi, M. Shabanian, F. Aryanasab, P. Zarrintaj, and M. Saeb, *Fire Mater.*, **42**, 914 (2018).
5. H. Vahabi, M. Shabanian, F. Aryanasab, R. Mangin, F. Laoutid, and M.R. Saeb, *Thermochim. Acta*, **666**, 51 (2018).
6. H. Vahabi, A. Raveshtian, M. Fasihi, R. Sonnier, M.R. Saeb, L. Dumazert, and B.K. Kandola, *Polym. Degrad. Stab.*, **143**, 164 (2017).
7. H. Vahabi, M.R. Saeb, K. Formela, and J.-M.L. Cuesta, *Prog. Org. Coat.*, **119**, 8 (2018).
8. H. Vahabi, M. Jouyandeh, M. Cochez, R. Khalili, C. Vagner, M. Ferriol, E. Movahedifar, B. Ramezanzadeh, M. Rostami, Z. Ranjbar, B.S. Hadavand, and M.R. Saeb, *Prog. Org. Coat.*, **123**, 160 (2018).
9. C. Naddeo, L. Vertuccio, G. Barra, and L. Guadagno, *Materials*, **10**, 943 (2017).
10. T.M. Hafshejani, A. Zamanian, J.R. Venugopal, Z. Rezvani, F. Sefat, M.R. Saeb, H. Vahabi, P. Zarrintaj, and M. Mozafari, *J. Control. Release*, **262**, 317 (2017).
11. H.A. Maddah, *Am. J. Poly. Sci.*, **6**, 1 (2016).
12. S. Zhang and A.R. Horrocks, *Prog. Polym. Sci.*, **28**, 1517 (2003).
13. N. Jha, A. Misra, and P. Bajaj, *J. Macromol. Sci. Rev. Macromol. Chem. Phys.*, **24**, 69 (1984).
14. C. Zhu, M. He, Y. Liu, J. Cui, Q. Tai, L. Song, and Y. Hu, *Polym. Degrad. Stab.*, **151**, 144 (2018).
15. C.A. Wilkie and A.B. Morgan, *Fire Retardancy of Polymeric Materials*, CRC Press, Boca Raton, FL, (2009).
16. T. Tang, X. Chen, H. Chen, X. Meng, Z. Jiang, and W. Bi, *Chem. Mater.*, **17**, 2799 (2005).
17. H. Wang, H. Niu, and J.-Y. Dong, *Polymer*, **126**, 109 (2017).
18. V. Ambrogi, P. Cerruti, C. Carfagna, M. Malinconico, V. Marturano, M. Perrotti, and P. Persico, *Polym. Degrad. Stab.*, **96**, 2152 (2011).
19. B. Kirschweng, K. Bencze, M. Sárközi, B. Hégely, G. Samu, J. Hári, D. Tátraaljai, E. Földes, M. Kállay, and B. Pukánszky, *Polym. Degrad. Stab.*, **133**, 192 (2016).
20. K. Doudin, S. Al-Malaika, H.H. Sheena, V. Tverezovskiy, and P. Fowler, *Polym. Degrad. Stab.*, **130**, 126 (2016).

21. H. Vahabi, M. Shabanian, F. Aryanasab, F. Laoutid, S. Benali, M.R. Saeb, F. Seidi, and B.K. Kandola, *Fire Mater.*, **42**, 593 (2018).
22. D. Marney, L. Russell, T. Soegeng, and V. Dowling, *J. Fire Sci.*, **25**, 471 (2007).
23. R. Pfaendner, *C. R. Chim.*, **9**, 1338 (2006).
24. X. Lai, J. Qiu, H. Li, R. Zhou, H. Xie, and X. Zeng, *J. Anal. Appl. Pyrolysis*, **120**, 361 (2016).
25. H. Chen, J. Wang, A. Ni, A. Ding, X. Han, and Z. Sun, *Materials*, **11**, 111 (2018).
26. K.A. Salmeia and S. Gaan, *Polym. Degrad. Stab.*, **113**, 119 (2015).
27. S. Wendels, T. Chavez, M. Bonnet, K.A. Salmeia, and S. Gaan, *Materials*, **10**, 784 (2017).
28. F. Qi, M. Tang, N. Wang, N. Liu, X. Chen, Z. Zhang, K. Zhang, and X. Lu, *RSC Adv.*, **7**, 31696 (2017).
29. Q. Ren, Y. Xia, X. Zhang, F. Zhang, J. Guo, and S. Zhang, *J. Macromol. Sci. B*, **57**, 31 (2018).
30. Z. Li and R. Yang, *Polym. Degrad. Stab.*, **109**, 233 (2014).
31. M. Rakotomalala, S. Wagner, and M. Döring, *Materials*, **3**, 4300 (2010).
32. A. Schäfer, S. Seibold, W. Lohstroh, O. Walter, and M. Döring, *J. Appl. Polym. Sci.*, **105**, 685 (2007).
33. M. Jouyandeh, S.M.R. Paran, A. Jannesari, and M.R. Saeb, *Prog. Org. Coat.*, **127**, 429 (2019).
34. Z. Karami, O.M. Jazani, A.H. Navarchian, and M.R. Saeb, *Prog. Org. Coat.*, **125**, 222 (2018).
35. T.S. Kermaniyan, H. Garmabi, and M.R. Saeb, *J. Appl. Polym. Sci.*, **135**, 46364 (2018).
36. E. Yarahmadi, K. Didehban, M.G. Sari, M.R. Saeb, M. Shabanian, F. Aryanasab, P. Zarrintaj, S.M.R. Paran, M. Mozafari, M. Rallini, and D. Puglia, *Prog. Org. Coat.*, **119**, 194 (2018).
37. M. Jouyandeh, Z. Karami, O.M. Jazani, K. Formela, S.M. R. Paran, A. Jannesari, M.R. Saeb, *Prog. Org. Coat.*, **126**, 129 (2019).
38. M. Jouyandeh, M. Shabanian, M. Khaleghi, S.M.R. Paran, S. Ghiyasi, H. Vahabi, K. Formela, D. Puglia, and M. R. Saeb, *Prog. Org. Coat.*, **125**, 384 (2018).
39. F. Memarian, A. Fereidoon, H.A. Khonakdar, S.H. Jafari, and M.R. Saeb, *Polym. Compos.*, **40**, 789 (2018).
40. M. Halvaee, K. Didehban, V. Goodarzi, M. Ghaffari, M. Ehsani, and M.R. Saeb, *J. Appl. Polym. Sci.*, **134**, 45389 (2017).
41. S. Vyazovkin, "Modern Isoconversional Kinetics: From Misconceptions to Advances," in *Handbook of Thermal Analysis and Calorimetry*, Vol. **6**, Elsevier Science B.V., London, 131 (2018).
42. T. Liavitskaya and S. Vyazovkin, *Macromol. Rapid Commun.*, **39**, 1700624 (2018).
43. S.M.R. Paran, H. Vahabi, M. Jouyandeh, F. Ducos, K. Formela, and M.R. Saeb, *J. Appl. Polym. Sci.*, **136**, 47483 (2019).
44. P. Das and P. Tiwari, *Thermochim. Acta*, **654**, 191 (2017).
45. M.R. Saeb, M. Ghaffari, H. Rastin, H.A. Khonakdar, F. Simon, F. Najafi, V. Goodarzi, P. Vijayan P., D. Puglia, F. H. Asl, and K. Formela, *RSC Adv.*, **7**, 2218 (2017).
46. H. Rastin, M.R. Saeb, M. Nonahal, M. Shabanian, H. Vahabi, K. Formela, X. Gabrion, F. Seidi, P. Zarrintaj, M. G. Sari, and P. Laheurte, *Prog. Org. Coat.*, **113**, 126 (2017).
47. M.G. Sari, H. Vahabi, X. Gabrion, P. Laheurte, P. Zarrintaj, K. Formela, M.R. Saeb, *Prog. Org. Coat.*, **119**, 171 (2018).
48. S. Vyazovkin, A.K. Burnham, J.M. Criado, L.A. Pérez-Maqueda, C. Popescu, and N. Sbirrazzuoli, *Thermochim. Acta*, **520**, 1 (2011).
49. H. Bockhorn, A. Hornung, and U. Hornung, *J. Anal. Appl. Pyrolysis*, **50**, 77 (1999).
50. P. Ptáček, T. Opravil, and F. Šoukal, *Ceram. Int.*, **42**, 16969 (2016).
51. N. Kongkaew, W. Pruksakit, and S. Patumsawad, *Energy Procedia*, **79**, 663 (2015).
52. S.M.R. Paran, H. Vahabi, F. Ducos, K. Formela, P. Zarrintaj, A. Laachachi, J.M. Lopez Cuesta, and M.R. Saeb, *J. Appl. Polym. Sci.*, **135**, 46488 (2018).
53. M. Nonahal, H. Rastin, M.R. Saeb, M.G. Sari, M. H. Moghadam, P. Zarrintaj, and B. Ramezanzadeh, *Prog. Org. Coat.*, **114**, 233 (2018).
54. M.G. Sari, M.R. Saeb, M. Shabanian, M. Khaleghi, H. Vahabi, C. Vagner, P. Zarrintaj, R. Khalili, S.M.R. Paran, B. Ramezanzadeh, and M. Mozafari, *Prog. Org. Coat.*, **115**, 143 (2018).
55. S. Ghiyasi, M.G. Sari, M. Shabanian, M. Hajibeygi, P. Zarrintaj, M. Rallini, L. Torre, D. Puglia, H. Vahabi, M. Jouyandeh, F. Laoutid, S.M.R. Paran, and M.R. Saeb, *Prog. Org. Coat.*, **120**, 100 (2018).
56. M.R. Saeb, H. Rastin, M. Nonahal, M. Ghaffari, A. Jannesari, and K. Formela, *J. Appl. Polym. Sci.*, **134**, 45221 (2017).
57. T. Wanjun, L. Yuwen, Z. Hen, W. Zhiyong, and W. Cunxin, *J. Therm. Anal. Calorim.*, **74**, 309 (2003).
58. M.E. Brown, M. Maciejewski, S. Vyazovkin, R. Nomen, J. Sempere, A. Burnham, J. Opfermann, R. Strey, H.L. Anderson, A. Kemmler, R. Keuleers, J. Janssens, H.O. Desseyn, C.-R. Li, T.B. Tang, B. Roduit, J. Malek, T. Mitsuhashi, *Thermochim. Acta*, **355**, 125 (2000).
59. E. Urbanovici, C. Popescu, and E. Segal, *J. Therm. Anal. Calorim.*, **58**, 683 (1999).
60. T. Damartzis, D. Vamvuka, S. Sfakiotakis, and A. Zabaniotou, *Bioresour. Technol.*, **102**, 6230 (2011).
61. R. Ebrahimi-Kahrizsangi and M. Abbasi, *Trans. Nonferrous Met. Soc. China*, **18**, 217 (2008).
62. E. Esmizadeh, M. Moghri, M.R. Saeb, M. Mohsen Nia, N. Nobakht, and N.P. Bende, *J. Vinyl Addit. Technol.*, **22**, 182 (2016).
63. A. François-Heude, E. Richaud, E. Desnoux, and X. Colin, *J. Photochem. Photobiol. A Chem.*, **296**, 48 (2015).
64. A. Imel, T. Malmgren, M. Dadmun, S. Gido, and J. Mays, *Biomaterials*, **73**, 131 (2015).
65. M. Schmid, A. Ritter, and S. Affolter, *J. Therm. Anal. Calorim.*, **83**, 367 (2006).
66. M.R. Saeb, H. Rastin, M. Nonahal, S.M.R. Paran, H.A. Khonakdar, and D. Puglia, *Prog. Org. Coat.*, **114**, 208 (2018).
67. M. Gamboiroža-Jukić and R. Čunko, *Acta Polym.*, **43**, 258 (1992).
68. C.L. Beyler and M.M. Hirschler, "Thermal Decomposition of Polymers," in *SFPE Handbook of Fire Protection Engineering*, Vol. **2**, Springer, Berlin, 111 (2002).
69. D.G. Papageorgiou, Z. Terzopoulou, A. Fina, F. Cuttica, G.Z. Papageorgiou, D.N. Bikiaris, K. Chrissafis, R.J. Young, I.A. Kinloch, *Composites Science and Technology*, **156**, 95 (2018).
70. H. Bockhorn, A. Hornung, U. Hornung, and D. Schawaller, *J. Anal. Appl. Pyrolysis*, **48**, 93 (1999).
71. S. Vyazovkin and N. Sbirrazzuoli, *Macromol. Rapid Commun.*, **27**, 1515 (2006).
72. D. Puglia, H. Rastin, M.R. Saeb, B. Shojaei, and K. Formela, *Prog. Org. Coat.*, **108**, 75 (2017).
73. P. Song, Y. Zhu, L. Tong, and Z. Fang, *Nanotechnology*, **19**, 225707 (2008).
74. F. Romani, R. Corrieri, V. Braga, and F. Ciardelli, *Polymer*, **43**, 1115 (2002).